Dalton Transactions

Time-Resolved and Steady-State Irradiation of Hydrophilic Sulfonated Bis-triazinyl-(bi)pyridines – Modelling Radiolytic Degradation

Journal:	*Dalton Transactions*
Manuscript ID	DT-ART-01-2019-000474.R1
Article Type:	Paper
Date Submitted by the Author:	05-Mar-2019
Complete List of Authors:	Horne, Gregory; Idaho National Laboratory, Center for Radiation Chemistry Research Mezyk, Stephen; California State University at Long Beach, Chemistry and Biochemistry Moulton, Nicole; California State University Long Beach, Chemistry and Biochemistry Peller, Julie; Valparaiso University College of Arts and Sciences, Chemistry Geist, Andreas; Karlsruher Institut für Technologie, Institut für Nukleare Entsorgung

ARTICLE

Time-Resolved and Steady-State Irradiation of Hydrophilic Sulfonated Bis-triazinyl-(bi)pyridines – Modelling Radiolytic Degradation

Received 00th January 20xx,
Accepted 00th January 20xx

DOI: 10.1039/x0xx00000x

Gregory P. Horne,*[a] Stephen P. Mezyk,[b] Nicole Moulton,[b] Julie R. Peller,[c] and Andreas Geist[d]

Efficient separation of the actinides from the lanthanides is a critical challenge in the development of a more sophisticated spent nuclear fuel recycling process. Based upon the slight differences in *f*-orbital distribution, a new class of soft nitrogen-donor ligands, the sulfonated bis-triazinyl-(bi)pyridines, has been identified and shown to be successful for this separation under anticipated, large-scale treatment conditions. The radiation robustness of these ligands is key to their implementation; however, current stability studies have yielded conflicting results. Here we report on the radiolytic degradation of the sulfonated 2,6-bis(1,2,4-triazine-3-yl)pyridine (BTP(S)) and 6,6'-bis(1,2,4-triazin-3-yl)-2,2'-bipyridine (BTBP(S)) in aerated, aqueous solutions using a combination of time-resolved pulsed electron techniques to ascertain their reaction kinetics with key aqueous radiolysis products (e_{aq}^-, $H^\bullet$, $^\bullet OH$, and $^\bullet NO_3$), and steady state gamma radiolysis in conjunction with liquid chromatography for identification and quantification of both ligands as a function of absorbed dose. These data were used to construct a predictive deterministic model to provide critical insight into the fundamental radiolysis mechanisms responsible for the ligands' radiolytic stability. The first-order decays of BTP(S) and BTBP(S) are predominantly driven by oxidative processes ($^\bullet OH$ and, to a lesser extent, H_2O_2), for which calculations demonstrate that the rate of degradation is inhibited by the formation of ligand degradation products that undergo secondary reactions with the primary products of water radiolysis. Overall, BTP(S) is ~20% more radiolytically stable than BTBP(S), but over 90% of either ligand is consumed within 1 kGy.

Introduction

Efficient separation of the *f*-elements from one another (4*f* lanthanides and 5*f* actinides) and from other elements is key to a sustainable future of advanced technologies and clean nuclear energy,[1-8] especially with environmental stewardship factors favouring recovery and recycling methods as opposed to continued geological exploitation. Further, the future of nuclear energy relies on minimizing nuclear waste whilst maximizing cost-effectiveness. These avenues of import are fulfilled by closing the nuclear fuel cycle, to harness the maximum energy content of uranium and plutonium based fuels, through the use of a more sophisticated spent nuclear fuel recycling process. Such a process needs to minimize the number of extraction cycles and solvent system constituents, while being able to separate all of the actinides from a given spent nuclear fuel matrix. This requires an efficient means of partitioning the trivalent actinides (An(III)) and lanthanides (Ln(III)), a particularly challenging separation owing to their chemical similarity.[9-12]

Despite their likeness, the An(III) exhibit sufficient covalent character in their metal-ligand bonds to facilitate selective complexation over the Ln(III).[13-16] This approach has been extensively studied, and has resulted in the synthesis of several hundred soft nitrogen- and sulphur-donor ligands for liquid-liquid separations.[17-21] Of these, the tridentate 2,6-bis(1,2,4-triazine-3-yl)pyridines (BTPs)[22-36] and the tetradentate 6,6'-bis(1,2,4-triazin-3-yl)-2,2'-bipyridines (BTBPs)[37-44] have shown most promise. Initially designed as hydrophobic extractants to support *Selective Actinide EXtraction* (SANEX)[46-48] from traditional *Plutonium Uranium Reduction EXtraction* (PUREX) process streams, they have recently been repurposed as hydrophilic complexants.[49,50] First lab-scale demonstration tests applying a hydrophilic BTP have successfully been performed, advancing the European *Innovative-SANEX* (*i*-SANEX)[55] and GANEX[56] concepts. Such processes provide an effective alternative to the *Trivalent Actinide Lanthanide Separation with Phosphorus-Reagent Extraction from Aqueous Komplexes* (TALSPEAK) process: wherein an acidic, hydrophobic organophosphorous complexant promotes co-extraction of all actinides and lanthanides into an organic phase, followed by an actinide-selective back-extraction using a hydrophilic polyaminocarboxylate ligand.[57,58] Recent *i*-SANEX approaches

[a] *Idaho National Laboratory, Center for Radiation Chemistry Research, Idaho Falls, ID, P.O. Box 1625, 83415, USA*
[b] *California State University Long Beach, Department of Chemistry and Biochemistry, Long Beach, CA 90804, USA.*
[c] *Valparaiso University, Department of Chemistry, Valparaiso, IN, 46383-6493, USA.*
[d] *Karlsruhe Institute of Technology (KIT), Institute for Nuclear Waste Disposal (INE), P.O. Box 3640, 76021 Karlsruhe, Germany.*
**E-mail: gregory.p.horne@inl.gov*
† Electronic Supplementary Information (ESI) available: kinetic plots for all investigated reaction kinetics. See DOI: 10.1039/x0xx00000x

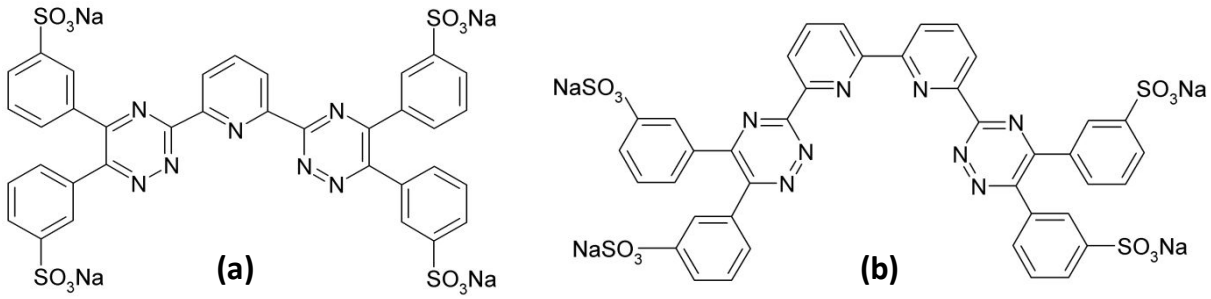

Figure 1. Chemical structures of **(a)** 2,6-bis[5,6-di(sulfonylphenyl)-1,2,4-triazin-3-yl] pyridine tetrasodium salt (BTP(S)) and **(b)** 6,6'-bis[5,6-di(3-sulfonylphenyl)-1,2,4-triazin-3-yl]-2,2'-bipyridine tetrasodium salt (BTBP(S)).

use a hydrophobic diglycolamide (tetraoctyldiglycolamide - TODGA)[59] for co-extraction of the An(III) and Ln(III), followed by An(III) recovery by water-soluble, hydrophilic derivatives of BTP or BTBP dissolved in dilute aqueous nitric acid (HNO_3). Tetrasulfonated BTBP, combined with TODGA, enable the back extraction of An(III) with high selectivity over Ln(III) (e.g., $SF_{Eu/Am} \approx 500–1000$) over a range of nitric acid concentrations (0.3 – 1 M) without the need for buffers,[49,51] which are critical for the restricted pH range (2 - 3) of the TALSPEAK process.

However, these hydrophilic derivatives need to be radiolytically robust, owing to the multi-component radiation field generated by the back-extracted An(III). The radiation chemistry of aqueous solutions is predominantly driven by the primary products of water radiolysis, given by reaction (**1**), where the numbers in brackets are the radiolytic yields of deposited energy (*G*-values μM J^{-1}) for species production.[60]

$$H_2O \rightsquigarrow [0.28]^{\bullet}OH + [0.06]H^{\bullet} + [0.27]e_{aq}^{-} + [0.05]H_2 + [0.07]H_2O_2 + [0.27]H_{aq}^{+} \quad (\mathbf{1})$$

The interaction of these primary radiolysis species with solutes dissolved in the aqueous phase of a typical solvent system lead to their degradation, thereby limiting the lifetime of a complexant as a function of its respective concentration and susceptibility to reaction. With respect to the tetrasulfonated derivatives of BTP and BTBP (BTP(S) and BTBP(S), respectively) shown in **Figure 1**, radiation testing has been limited to a handful of conflicting studies. Galan *et al*. investigated the stability of 10 mM BTP(S) dissolved in 0.5 M HNO_3 as a function of steady-state gamma (γ-) irradiation (50 to 1000 kGy).[61] Under dilute HNO_3 conditions the key radiolysis products are the hydroxyl radical ($^{\bullet}OH$, $E^o = 2.7$ V)[74], hydrogen peroxide (H_2O_2, $E^o = 1.8$ V), nitrous acid (HNO_2, $E^o = 0.984$ V), and, to a lesser extent, the hydrogen atom ($H^{\bullet}$, $E^o = -2.3$ V)[74] and nitrate radical ($^{\bullet}NO_3$, $E^o = 2.3 – 2.6$ V)[62], generalized by the following reactions:[63-68]

$$e^{-} \xrightarrow{110\ fs} e_{pre}^{-} \xrightarrow{240\ fs} e_{aq}^{-} \quad (\mathbf{2})$$

$$e_{pre}^{-} + H_{aq}^{+} \rightarrow H^{\bullet} \qquad k = 2.2 \times 10^{12}\ M^{-1}\ s^{-1} \quad (\mathbf{3})$$

$$e_{aq}^{-} + H_{aq}^{+} \rightarrow H^{\bullet} \qquad k = 2.3 \times 10^{10}\ M^{-1}\ s^{-1} \quad (\mathbf{4})$$

$$NO_3^{-} + e_{pre}^{-} \rightarrow \ldots \rightarrow HNO_2 \qquad k = 1.0 \times 10^{13}\ M^{-1}\ s^{-1} \quad (\mathbf{5})$$

$$NO_3^{-} + e_{aq}^{-} \rightarrow \ldots \rightarrow HNO_2 \qquad k = 9.7 \times 10^{9}\ M^{-1}\ s^{-1} \quad (\mathbf{6})$$

$$NO_3^{-} + H^{\bullet} \rightarrow \ldots \rightarrow HNO_2 \qquad k = 1.0 \times 10^{7}\ M^{-1}\ s^{-1} \quad (\mathbf{7})$$

$$HNO_3 + {}^{\bullet}OH \rightarrow {}^{\bullet}NO_3 + H_2O \qquad k = 1.9 \times 10^{7}\ M^{-1}\ s^{-1} \quad (\mathbf{8})$$

$$HNO_2 + H_2O_2 \rightarrow NO_3^{-} + H_2O + H_{aq}^{+} \quad k = 1.9 \times 10^{7}\ M^{-1}\ s^{-1} \quad (\mathbf{9})$$

Galan *et al*. reported significant ligand degradation, with ~90% of BTP(S) consumed within 250 kGy.[61] However, ligand degradation was indirectly followed using ^{241}Am and ^{152}Eu distribution ratios, established upon contacting the irradiated BTP(S) solutions with an unirradiated organic phase: 0.2 M TODGA/5% 1-octanol/kerosene. This approach does not account for the potential of BTP(S) degradation products being soluble in the organic phase and coordinating Am(III), thereby distorting $^{241}Am/^{152}Eu$ distribution ratios, especially considering the complexing nature of the hydrophobic/lipophilic BTPs and BTBPs.[22-44] This is supported by their observation of a sulphurous odour for absorbed gamma doses ≥200 kGy, and detection of the loss of the water solubilizing sulphonate functional groups. Further, no quantitative mechanistic explanation/interpretation was provided for the radiolytic degradation of BTP(S), which is paramount for the design of predictive computer models to inform process design.

Peterman *et al.* employed a more applied approach using a bespoke solvent irradiation test loop to assess the performance of BTP(S) under envisioned *i*-SANEX process conditions: 18 mM BTP(S) in 0.35 M HNO_3 irradiated in contact with a 0.2 M TODGA/5% 1-octanol/*n*-dodecane organic phase.[69] In contrast to previous work, no significant BTP(S) degradation up to doses of 175 kGy was reported – indirectly determined by distribution ratios of ^{241}Am, ^{139}Ce, and $^{152/154}Eu$ – despite the measurement of increasing dissolved sulphate concentration with absorbed γ-dose. Thus, BTP(S) degradation was found to have little impact upon the performance of the *i*-SANEX process. However, no explanation has yet been provided to account for the disparity between the two irradiation studies, beyond the qualitative invocation of biphasic media and constant dissolved oxygen completely altering single phase radiation chemistry. Firstly, the presence of an additional less-dense phase adds the complexities of mass transfer and the formation of additional degradation products. However, time-resolved experiments would provide critical insight as to whether such competition kinetics is likely to affect the presumed array of reactions responsible for BTP(S) degradation. Secondly, with or without dissolved oxygen (~0.25 mM in aqueous solutions), the presence of the nitrate anion (NO_3^-) affords the same effect, i.e., inhibition of the hydrated electron (e_{aq}^-, $E^o = -2.9$ V) and $H^{\bullet}$

chemistries. Compare reactions (**5**), (**6**), and (**7**) with the following:

$O_2 + e_{aq}^- \rightarrow O_2^{\bullet -}$ $k = 1.9 \times 10^{10}$ M^{-1} s^{-1} (**10**)

$O_2 + H^\bullet \rightarrow HO_2^\bullet$ $k = 1.2 \times 10^{10}$ M^{-1} s^{-1} (**11**)

Despite the importance of performing experiments under as realistic a scenario as possible, the absence of quantitative mechanistic insight afforded by more fundamental studies negates the ability to assemble reaction sets for inclusion in predictive computer models that can accommodate/respond to changes in solvent system formulation, thereby affording a more effective assessment of process system performance and development.

In light of conflicting studies, absence of direct ligand degradation measurements, and sound mechanistic interpretation, we report a thorough characterization of the radiolytic degradation of BTP(S) and BTBP(S) in aerated, single-phase, aqueous solutions using a combination of: (i) time-resolved pulsed electron techniques to ascertain the reaction kinetics of both ligands with key aqueous radiolysis products (e_{aq}^-, $H^\bullet$, $^\bullet OH$, and $^\bullet NO_3$); and (ii) steady state γ-radiolysis in conjunction with liquid chromatographic techniques for identification and quantification of both ligands as a function of absorbed dose. The data were used to construct a predictive deterministic model to provide critical insight into the fundamental radiolysis mechanisms responsible, providing a baseline from which future studies can extrapolate to more complex systems, e.g. dilute HNO_3 or biphasic *i*-SANEX conditions.

Experimental

Materials

2,6-bis[5,6-di(3-sulfonylphenyl)-1,2,4-triazin-3-yl] pyridine tetrasodium salt (BTP(S), *98% Technocomm Ltd*), 6,6'-bis[5,6-di(3-sulfonylphenyl)-1,2,4-triazin-3-yl]-2,2'-bipyridine tetrasodium salt (BTBP(S), synthesised according to[51,70]), potassium thiocyanate (KSCN, *≥99.0% ACS Reagent Grade, Sigma-Aldrich*), tertiary butanol (tBuOH, *≥99.5% Sigma Aldrich*), and nitric acid (HNO_3, *≥99.999% Trace Metals Basis Sigma-Aldrich*) were used as received without further purification. Ultra-pure water (≥ 18.2 MΩ) was used for all aqueous solutions.

Irradiations

Steady-State. Gamma irradiations were performed using a Nordion Gammacell 220 and a Shepherd 109-68 cobalt-60 irradiator unit at the Notre Dame Radiation Laboratory (NDRL). Samples consisted of 50 mL aerated aqueous stock solutions of each ligand irradiated in a sealed screw-cap glass vessel. At specific absorbed gamma dose intervals, samples were extracted for quantification of BTP(S) or BTBP(S). Dosimetry was determined using Fricke solution,[71] subsequently corrected for ^{60}Co decay ($\tau^1/_2$ = 5.27 years), affording a dose rate of 0.017 and 0.313 Gy s^{-1}, for the Nordion and Shepherd irradiator units, respectively.

Time-Resolved. Reaction kinetics were determined using the NDRL nanosecond pulsed electron linear accelerator facility. A detailed description of the irradiation procedure and transient absorption detection system has been given previously.[72,73] Dosimetry was determined using N_2O saturated solutions of 10 mM KSCN at λ_{max} = 472 nm ($G\varepsilon = 5.2 \times 10^{-4}$ m^2 J^{-1}).[74] Isolation and reaction kinetics of specific radicals were achieved using the following conditions:

- *Hydrated Electron (e_{aq}^-)*. Direct decay kinetics observed at 720 nm using N_2 saturated aqueous solutions of 0.5 M tBuOH and 10 mM phosphate buffer at pH 7.01 for both compounds.
- *Hydrogen Atom ($H^\bullet$)*. Direct growth kinetics of the BTP(S)/BTBP(S) transients observed at the peak transient absorbances of 400 and 420 nm, respectively, using N_2 saturated solutions containing 20 mM tBuOH and 10 mM phosphate buffer at pH 2.0.
- *Hydroxyl Radical ($^\bullet OH$)*. Direct growth kinetics of the BTP(S)/BTBP(S) transient observed at 400 nm for both species, using N_2O saturated solutions of 10 mM phosphate buffer at pH 7.00.
- *Nitrate Radical ($^\bullet NO_3$)*. Direct decay kinetics observed at 630 nm using N_2O saturated aqueous solutions of 6.0 M HNO_3 for both compounds

All transient absorption measurements were made using a 1.0 cm optical pathlength quartz flow cell, with flow rate and temperature regulated to ensure that each electron pulse irradiated a fresh sample. Solution temperatures were directly measured by an in-flow thermocouple placed immediately above the irradiation cell. The temperature stability of the system was better than ±0.3 °C. Kinetic traces were generated through averaging 8–16 individual measurements. Quoted errors for the reaction rate coefficients are a combination of measurement precision and sample concentration errors.

Quantification

Liquid chromatography-mass spectrometry (LCMS) analysis was performed at Valparaiso University using a Waters™ Acquity UPLC H-class system equipped with a QDa detector. Chromatographic separations were performed with a Waters™ Acquity UPLC BEH C18 column (1.7 µm, 2.1 × 50 mm) and a gradient flow beginning with 10% acetonitrile (0.1% formic acid) and 90% water (0.1% formic acid), changing to 60% acetonitrile and 40% water at 4.0 minutes. The solvent returned to the initial formulation at 6.0 minutes. The solvent flow rate was 0.23 mL min^{-1}, with the column and sample compartment temperatures held constant at 20 °C. Mass spectrometry was utilized in positive scan mode, with a cone voltage of 15 V and a capillary voltage of 1.5 kV. BTP(S) and BTBP(S) were detected and analysed using selected ion recording (SIR) at m/z = 862 and 939, respectively. Degradation products were observed for BTP(S) at m/z = 438, and for BTBP(S) at m/z = 515, 543, and 572. Quantification was not possible as

their structures were not characterized, and thus standards were not able to be prepared.

Reaction Kinetics Modelling

Deterministic calculations were performed to model the reaction kinetics of the above systems. Reactions are expressed as a series of coupled ordinary differential equations and solved using the FACSIMLE numerical algorithm (MCPA software). The chemical reaction set reflects water radiolysis compilations by Buxton *et al.*[60] and Elliot and Bartels,[75] and experimental reaction kinetics determined in this work. Where experimental data were absent, optimised kinetic parameters were calculated.

Table 1. Rate coefficients for the reaction of BTP(S) and BTBP(S) with e_{aq}^-, H•, •OH, and •NO_3.

Ligand	Rate Coefficient (*k*) (10^9 M^{-1} s^{-1})			
	e_{aq}^-	H•	•OH	•NO_3
BTP(S)	16.0 ± 0.2	3.07 ± 0.11	2.48 ± 0.14	(3.72 ± 0.13) × 10^{-2}
BTBP(S)	7.98 ± 0.26	5.20 ± 0.18	4.24 ± 0.05	(1.04 ± 0.07) × 10^{-2}

Results and Discussion

Reaction Kinetics

The free-radical induced radiolytic degradation of BTP(S) and BTBP(S) in the aqueous phase may be driven by reduction, through e_{aq}^- and H• reactions, and/or oxidation by •OH, and •NO_3 radicals. To elucidate their respective reactivity, time-resolved nanosecond pulse radiolysis was performed to determine reaction rate coefficient values. All four radical species were found to react with BTP(S) and BTBP(S), the rate coefficients for which are given in **Table 1**. Typical data for the reaction of •OH with the sulfonated bis-triazinyl-(bi)pyridines are shown in **Figure 2**. Analogous data for the remaining transients can be found in Supplementary Information.

Reaction of the •OH, e_{aq}^-, and H• are all fast, ca. 5 × 10^9 M^{-1} s^{-1} at room temperature. The slightly greater reactivity of •OH and H• for the BTBP(S) compound, plus the transient absorption spectra obtained, indicate that these radicals are adding to the extended conjugated system of these molecules.[60] For the •NO_3 radical, significantly lower reactivity

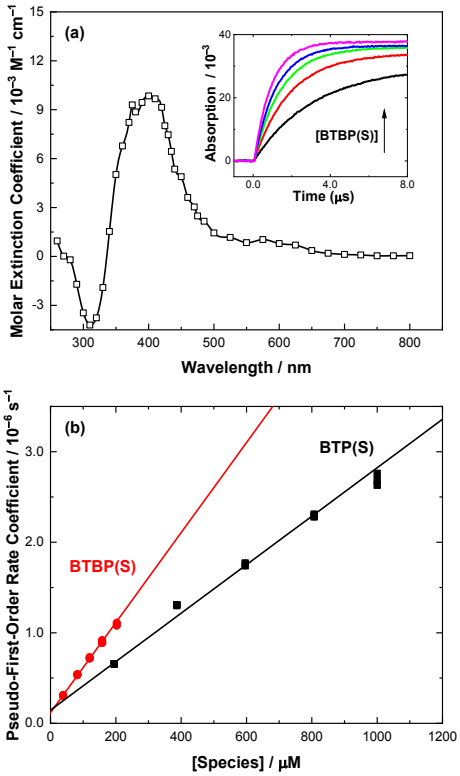

Figure 2. (a) Transient spectra for the oxidation product of the hydroxyl radical reaction with BTBP(S) for 202.6 μM BTBP(S). Spectral intensity measured at the end of kinetic growth (~5-6 μs after pulse, see *Inset*). *Inset*: kinetic growth behaviour in pH 7.02, N_2O-saturated aqueous solution at 22.2 °C in the presence of 38.5 (**Black**), 82.3 (**Red**), 120.3 (**Green**), 158.1 (**Blue**), and 202.6 (**Magenta**) μM BTBP(S). **(b)** Second-order determination of the rate coefficient for the hydroxyl radical reaction with BTP(S)(■) and BTBP(S)(●), based upon pseudo-first-order exponential growth fits to raw kinetic data. Solid lines are weighted linear fits, with slopes corresponding to the second-order rate coefficient: $k_{BTP(S)}$ = (2.48 ± 0.14) × 10^9 M^{-1} s^{-1} and $k_{BTBP(S)}$ = (4.24 ± 0.05) × 10^9 M^{-1} s^{-1}.

is measured for both ligands, suggesting an abstraction reaction (either electron abstraction from one of the sulphur atoms, or hydrogen atom abstraction) occurs instead. The absolute molar extinction coefficient (ε) values (M^{-1} cm^{-1}) plotted for the transient spectra obtained for these radicals' reactions were calculated using standard cooperative scavenging yield equations.[76]

Ligand Degradation Rates

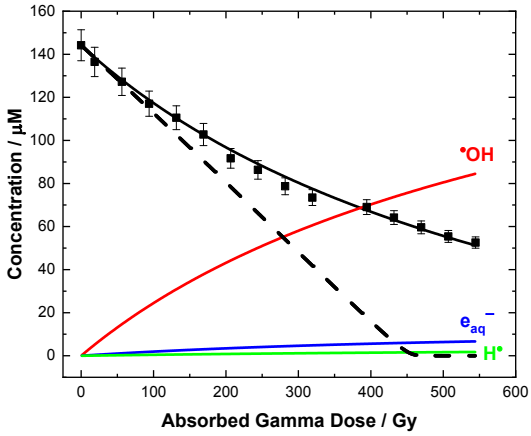

Figure 3. Gamma radiolysis of BTP(S) (■) as a function of absorbed gamma dose. Curves are from deterministic reaction kinetics calculations predicting the change in concentration of: BTP(S) without secondary degradation product reactions with •OH (**Dashed Black**); and with secondary degradation product reactions with •OH (**Solid Black**) and the cumulative reaction concentrations of BTP(S) with •OH (**Solid Red**), e_{aq}^- (**Solid Blue**), and H• (**Solid Green**).

Both BTP(S) and BTBP(S) exhibit first-order decay kinetics, affording dose constants[77] of -1.84 and -2.24 × 10^{-3} Gy^{-1}, respectively. BTBP(S) degrades ~20% faster than BTP(S) in water. This effect may be rationalized by considering its higher rate coefficient (**Table 1**) for the reducing products of water radiolysis, i.e. e_{aq}^- and H•. However, modelling these systems provides significantly greater insight into the fundamental reaction mechanisms contributing to total ligand degradation. The radiolytic degradation of BTP(S) and BTBP(S) as a function of absorbed γ-dose are given in **Figure 3** and **Figure 4**, respectively. These data demonstrate that <600 Gy is needed to have significant BTP(S) and BTBP(S) degradation. Although quantitative comparison to large-scale conditions is difficult, as reprocessing radiolytic doses depend strongly on fuel burnup and cooling times, these low dose values are consistent with previous calculations of dose-rates and doses experienced by a SANEX solvent (up to 800 Gy/h for MOX-45 fuel).[78] However, these ligands are designed to recover An(III) following their separation from the bulk of short-lived fission products, and are not intended for recycle. Consequently, envisioned dose rates are expected to be much lower. Calculations show that ligand degradation is predominantly driven by oxidative processes (•OH and, to a lesser extent, H_2O_2), owing to the aerated conditions ($[O_2]$ = 0.25 mM) of these experiments. Scavenging by O_2, reactions (**10**) and (**11**), renders contributions to total ligand degradation by the reducing products of water radiolysis negligible.

For BTP(S), **Figure 3**, ~90% of total degradation is through reaction with •OH, and the remainder with e_{aq}^- (~7%) and H• (~2%). However, the extent of BTP(S) radiolysis is inhibited by the formation of its own degradation products. Without competing secondary processes, •OH consumes BTP(S) at a significantly faster rate (0.32 µM Gy^{-1}), demonstrated by the dashed black line in **Figure 3**. This zeroth-order kinetic

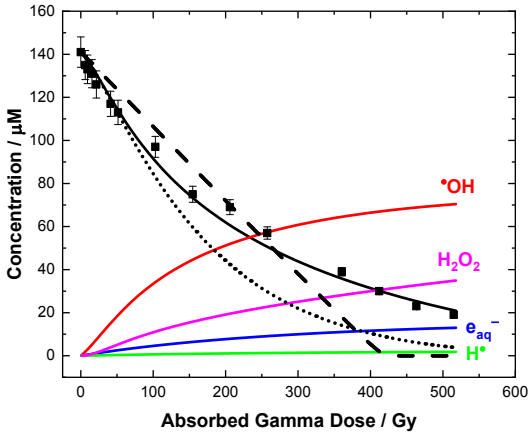

Figure 4. Gamma radiolysis of BTBP(S) (■) as a function of absorbed gamma dose. Curves are from deterministic reaction kinetics calculations predicting the change in concentration of: BTBP(S) without secondary degradation product reactions (**Dashed Black**); with BTBP(S) + H_2O_2 (**Dotted Black**); and with BTBP(S) + H_2O_2 and secondary degradation product reactions with •OH and H_2O_2 (**Solid Black**) and the cumulative reaction concentrations of BTP(S) with •OH (**Solid Red**), e_{aq}^- (**Solid Blue**), H• (**Solid Green**), and H_2O_2 (**Solid Magenta**).

behaviour is not observed experimentally, and is indicative of competing processes. Considering the number of aromatic constituents possessed by BTP(S), it is not unreasonable to imagine a single BTP(S) molecule undergoing sequential reactions with •OH, thereby preserving the integrity of other BTP(S) molecules, and thus minimizing total ligand degradation. This effect has been postulated previously for other compounds containing aromatic moieties.[79] By including sequential •OH reactions, using rate coefficients equal to or of the order of that for *k*(BTP(S) + •OH), near perfect agreement can be obtained between experiment and calculation, as shown by the solid black line, lending support to this mechanistic interpretation.

With regards to BTBP(S), **Figure 4**, its faster rate of degradation cannot be attributed to its higher affinity for the reducing products of water radiolysis due to the action of dissolved O_2, reactions (**10**) and (**11**). This observation suggests that BTBP(S) is subject to additional chemistries. Modelling this system using the associated experimentally determined rate coefficients in **Table 1** affords the zeroth-order dashed black line in **Figure 4**. This calculation highlights not only the need for sequential degradation product reactions, but also the existence of additional BTBP(S) radiolysis pathways, as the initial rate of degradation is faster than that attainable using the

available transient products of water radiolysis, i.e., e_{aq}^-, $H^\bullet$, and $^\bullet OH$. Agreement can only be attained if BTBP(S) can react with H_2O_2, a stable/steady-state molecular water radiolysis product, outlined by reaction (**12**).

$$\text{BTBP(S)} + H_2O_2 \rightarrow \text{BTBP(S)}(\text{-H}^\bullet) + {}^\bullet OH + H_2O \qquad k \sim 250\ M^{-1}\ s^{-1} \qquad (\mathbf{12})$$

$$e_{aq}^- + H_2O_2 \rightarrow {}^\bullet OH + OH^- \qquad k = 1.2 \times 10^{10}\ M^{-1}\ s^{-1} \qquad (\mathbf{13})$$

Inclusion of this process allows for the initial rate of BTBP(S) degradation to be attained, as shown by the dotted black curve in **Figure 4**. Agreement with experiment, given by the solid black line, is achieved by incorporating sequential degradation product reactions for both $^\bullet OH$ and H_2O_2, in the same manner as for BTP(S). Overall, the degradation of BTBP(S) within the experimental window can be attributed to $^\bullet OH$ (~58%), H_2O_2 (~29%), e_{aq}^- (~11%), and $H^\bullet$ (~2%). The slightly higher contribution from e_{aq}^-, relative to BTP(S) radiolysis, is a consequence of BTBP(S) scavenging H_2O_2, thereby inhibiting reaction (**13**) and freeing up e_{aq}^- for partitioning between BTBP(S) and O_2.[80]

Conclusions

In summary, a fundamental investigation into the radiolytic degradation of the sulfonated bis-triazinyl-(bi)pyridines, BTP(S) and BTBP(S), has directly and quantitatively established the key processes responsible for their radiolysis and their associated reaction kinetic mechanisms, validated by a predictive deterministic model. Oxidative processes, predominantly driven by $^\bullet OH$ chemistry, leads to first-order decay of both ligands, the rate of which is progressively inhibited by the formation of reactive BTP(S)/BTBP(S) degradation products. For concentrations investigated here (~145 µM), over 90% of both ligands are consumed within 1 kGy, contrary to previous studies under envisioned applied *i*-SANEX conditions, i.e., dilute HNO_3 contacted with 0.2 M TODGA/5% 1-octanol dissolved in an organic diluent. With respect to dilute HNO_3 solutions,[61] conversion of $^\bullet OH$ to $^\bullet NO_3$ may provide some explanation as to why significantly higher doses (~250 kGy) were required for a similar extent of ligand degradation, as $^\bullet NO_3$ reacts approximately two orders of magnitude slower with BTP(S) and BTBP(S). The absence of significant ligand degradation in biphasic systems,[69] is likely a consequence of mass transfer of organic phase species scavenging both $^\bullet OH$ and $^\bullet NO_3$, thereby inhibiting degradation. However, until the radiolytic behaviour of these two ligands is investigated in a similar manner as here for dilute HNO_3 and biphasic conditions, their current level of radiolytic robustness is unknown for an applied process. Further, although BTP(S) and BTBP(S) degradation product parameter optimization is sufficient for the purposes of this study, evaluation of the presented modelling reaction scheme would benefit from isolation and synthesis of the associated degradation products in conjunction with respective reaction kinetics studies.

Process viability of both ligands would be enhanced by substituting their sulphur content with carboxylate functionality, thereby conforming to the CHON (carbon, hydrogen, oxygen, and nitrogen) principle, facilitating clean disposal by incineration.[81,82] Such compounds are now being readily synthesised, for which preliminary experiments have been performed, yielding similar reaction kinetics and radiolytic behaviour as their sulfonated counterpart – discussed in a follow-up article.

Conflicts of interest

There are no conflicts to declare.

Acknowledgements

This research has been funded by the US-DOE Assistant Secretary for NE, under the Material Recovery and Waste Form Development Campaign, DOE-Idaho Operations Office Contract DE-AC07-05ID14517 and DE-NE0008406 Nuclear Energy Universities Program (NEUP) grant. The gamma and pulsed electron irradiations reported herein were performed at the Notre Dame Radiation Laboratory (NDRL). The NDRL is supported by the Division of Chemical Sciences, Geosciences and Biosciences, Basic Energy Sciences, Office of Science, United States Department of Energy (DOE) through Award No. DE-FC02-04ER15533.

The authors would like to thank the DOE-SACSESS and DOE-GENIORS collaboration for supporting this research effort.

Notes and references

(1) J. Lucas, P. Lucas, T. Le Mercier, A. Rollat, W. Davenport, *Rare Earths. Science, Technology, Production, and Use*, Elsevier, Amsterdam, **2015**.
(2) S. Cotton, *Lanthanide and Actinide Chemistry*, John Wiley & Sons, Ltd., Chichester, England, **2006**.
(3) National Research Council, *Managing Materials for a Twenty-first Century Military*, The National Academies Press, Washington, DC, USA, **2008**. Available at: https://doi.org/10.17226/12028.
(4) J. -C. G. Bünzli, *Chem. Rev.* 2010, **110 (5)**, 2729.
(5) M. C. Heffern, L. M. Matosziuk, and T. J. Meade, Imaging *Chem. Rev.* 2014, **114 (8)**, 4496.
(6) A. J. Amoroso and S. J. A. Pope, *Chem. Soc. Rev.* 2015, **44**, 4723.
(7) E. W. Price and C. Orvig, *Chem. Soc. Rev.* 2014, **43**, 260.
(8) P. D. Wilson, *The Nuclear Fuel Cycle: From Ore to Waste*, Oxford University Press, Oxford, NY, USA, 1996.
(9) G. T. Seaborg, *Radiochim. Acta*, 1993, **61**, 115.
(10) S. Cotton, Comprehensive Coordination Chemistry II, ed. J. A. McCleverty and T. J. Meyer, Elsevier, Oxford, 2004, vol. 3, pp. 93–188.
(11) C. J. Burns, M. P. Neu, H. Boukhalfa, K. E. Gutowski, N. J. Bridges, and R. D. Rogers, Comprehensive Coordination Chemistry II, ed. J. A. McCleverty and T. J. Meyer, Elsevier: Oxford, 2004, vol. 3, pp. 189–332.
(12) J. J. Katz, L. R. Morss, N. M. Edelstein, J. Fuger, The Chemistry of the Actinide and Transactinide Elements, ed. J. J. Katz, L. R. Morss, N. M. Edelstein and J. Fuger, Springer, Dordrecht, 2006, vol. 1, pp. 1–17.
(13) G. R. Choppin, *J. Alloys Compd.*, 1995, **223**, 174.
(14) Alexander, V. Design and Synthesis of Macrocyclic Ligands and Their Complexes of Lanthanides and Actinides. *Chem. Rev.*, 1995, 95, 273–342.
(15) G. R. Choppin, *J. Alloys Compd.*, 2002, **344**, 55.
(16) A. J. Gaunt and M. P. Neu, C. R. Chim., 2010, **13**, 821.
(17) C. Ekberg, A. Fermvik, T. Retegan, G. Skarnemark, M. R. S. Foreman, M. J. Hudson, S. Englund, and M. Nilsson, *Radiochim. Acta*, 2008, **96**, 225.
(18) Z. Kolarik, *Chem. Rev.*, 2008, **108**, 4208.
(19) F. W. Lewis, M. J. Hudson, and L. M. Harwood, *Synlett*, 2011, **18**, 2609.
(20) M. J. Hudson, L. M. Harwood, D. M. Laventine, and F. W. Lewis, *Inorg. Chem.*, 2013, **52**, 3414.
(21) P. J. Panak and A. Geist, *Chem. Rev.*, 2013, **113**, 1199.
(22) Z. Kolarik, U. Mullich, and F. Gassner, *Solvent Extr. Ion Exch.*, 1999, **17**, 1155.
(23) M. G. B. Drew, D. Guillaneux, M. J. Hudson, P. B. Iveson, M. L. Russell, and C. Madic, *Inorg. Chem. Commun.*, 2001, **4**, 12.
(24) P. B. Iveson, C. Riviere, D. Guillaneux, M. Nierlich, P. Thuery, M. Ephritikhine, and C. Madic, *Chem. Commun.*, 2001, 1512.
(25) C. Boucher, M. G. B. Drew, P. Giddings, L. M. Harwood, M. J. Hudson, P. B. Iveson, and C. Madic, *Inorg. Chem. Commun.*, 2002, **5**, 596.
(26) G. Ionova, C. Rabbe, R. Guillaumont, S. Ionov, C. Madic, J, -C Krupa, and D. Guillaneux, *New J. Chem.*, 2002, **26**, 234.
(27) J. -C. Berthet, Y. Miquel, P. B. Iveson, M. Nierlich, P. Thuery, C. Madic, and M. Ephritikhine, *J. Chem. Soc., Dalton Trans.*, 2002, 3265.
(28) S. Colette, B. Amekraz, C. Madic, L. Berthon, G. Cote, and C. Moulin, *Inorg. Chem.*, 2002, **41 (26)**, 7031.
(29) S. Colette, B. Amekraz, C. Madic, L. Berthon, G. Cote, and C. Moulin, *Inorg. Chem.*, 2003, **42 (7)**, 2215.
(30) S. Colette, B. Amekraz, C. Madic, L. Berthon, G. Cote, and C. Moulin, *Inorg. Chem.*, 2004, **43 (21)**, 6745.
(31) M. A. Denecke, A. Rossberg, P. J. Panak, M. Weigl, B. Schimmelpfennig, and A. Geist, *Inorg. Chem.*, 2005, **44**, 8418.
(32) M. G. B. Drew, M. R. S. J. Foreman, A. Geist, M. J. Hudson, F. Marken, V. Norman, and M. Weigl, *Polyhedron*, 2006, **25**, 888.
(33) M. Steppert, C. Walther, A. Geist, and T. Fanghanel, *New J. Chem.*, 2009, **33**, 2437.
(34) N. L. Banik, B. Schimmelpfennig, C. M. Marquardt, B. Brendebach, A. Geist, and M. A. Denecke, *Dalton Trans.*, 2010, **39**, 5117.
(35) G. Benay, R. Schurhammer, and G. Wipff, *Phys. Chem. Chem. Phys.*, 2010, **12**, 11089.
(36) S. Trumm, A. Geist, P. J. Panak, and T. Fanghanel, *Solvent Extr. Ion Exch.*, 2011, **29 (2)**, 213.
(37) M. G. B. Drew, M. R. S. J. Foreman, C. Hill, M. J. Hudson, and C. Madic, *Inorg. Chem. Commun.*, 2005, **8**, 239.
(38) M. Nilsson, C. Ekberg, M. Foreman, M. Hudson, J. -O. Liljenzin, G. Modolo, and G. Skarnemark, *Solvent Extr. Ion Exch.*, 2006, **24 (6)**, 823.
(39) V. Hubscher-Bruder, J. Haddaoui, S. Bouhroum, and F. Arnaud-Neu, *Inorg. Chem.*, 2010, **49**, 1363.
(40) C. Ekberg, E. Aneheim, A. Fermvik, M. Foreman, E. Lofstrom-Engdahl, T. Retegan, and I. Spendlikova, *J. Chem. Eng. Data*, 2010, **55**, 5133.
(41) J. -C. Berthet, J. Maynadie, P. Thuery, and M. Ephritikhine, *Dalton Trans.*, 2010, **39**, 6801.

(42) L. M. Harwood, F. W. Lewis, M. J. Hudson, J. John, and P. Distler, *Solvent Extr. Ion Exch.*, 2011, **29**, 551.
(43) F. W. Lewis, L. M. Harwood, M. J. Hudson, P. Distler, J. John, K. Stamberg, A. Nunez, H Galan, and A. G. Espartero, *Eur. J. Org. Chem.*, 2012, 1509.
(44) E. Aneheim, B. Gruner, C. Ekberg, M. R. S. J. Foreman, Z. Hajkova, E. Lofstrom-Engdahl, M. G. B. Drew, and M. J. Hudson, *Polyhedron*, 2013, **50**, 154.
(45) A. Geist, C. Hill, G. Modolo, M. R. S. Foreman, M. Weigl, K. Gompper, M. J. Hudson, and C. Madic, *Solvent Extr. Ion Exch.,* 2006, **24,** 463.
(46) C. Madic, M. J. Hudson, J. -O; Liljenzin, J. -P. Glatz, R. Nannicini, A. Facchini, Z. Kolarik, and R. Odoj, *Prog. Nucl. Energy*, 2002, **40**, 523.
(47) C. Madic, B. Boullis, P. Baron, F. Testard, J. Hudson, J. -O. Liljenzin, B. Christiansen, M. Ferrando, A. Facchini, A. Geist, G. Modolo, A. G. Espartero, and J. de Mendoza, *J. Alloys Compd.*, 2007, **44-445**, 23.
(48) S. Bourg, C. Hill, C. Caravaca, C. Rhodes, C. Ekberg, R. Taylor, A. Geist, G. Modolo, L. Cassayre, R. Malmbeck, M. Harrison, G. de Angelis, A. Espartero, S. Bouvet, and N. Ouvrier, *Nucl. Eng. Des.*, 2011, **241**, 3427.
(49) A. Geist, U. Mullich, D. Magnusson, P. Kaden, G. Modolo, A. Wilden, and T. Zevaco, *Solv. Extr. Ion Exch.*, 2012, **30**, 433.
(50) F. W. Lewis, L. M. Harwood, M. J. Hudson, A. Geist, V. N. Kozhevnikov, P. Distler, and J. John, *Chemical Science*, 2015, **6**, 4812.
(51) C. Wagner, U. Müllich, A. Geist, and P. J. Panak, *Solvent Extr. Ion Exch.,* 2016, 34, 103.
(52) A. Wilden, G. Modolo, P. Kaufholz, F. Sadowski, S. Lange, M. Sypula, D. Magnusson, U Mullich, A. Geist, and D. Bosbach, *Solv. Extr. Ion Exch*., 2015, **33**, 91.
(53) M. Carrott, K. Bell, J. Brown, A. Geist, C. Gregson, X. Hérès, C. Maher, R. Malmbeck, C. Mason, G. Modolo, U. Müllich, M. Sarsfield, A. Wilden, and R. Taylor, *Solvent Extr. Ion Exch.,* 2014, 32, 447.
(54) R. Malmbeck, D. Magnusson, S. Bourg, M. Carrott, A. Geist, X. Hérès, M. Miguirditchian, G. Modolo, U. Müllich, C. Sorel, R. Taylor, and A. Wilden, *Radiochim. Acta* 2019, *(submitted)*.
(55) X. Hérès, C. Sorel, M. Miguirditchian, B. Camès, C. Hill, I. Bisel, D. Espinoux, C. Eysseric, P. Baron, and B. Lorrain, Results of recent counter-current tests on An(III)/Ln(III) separation using TODGA extractant. In *Proc. Internat. Conf. GLOBAL 2009 (The Nuclear Fuel Cycle: Sustainable Options & Industrial Perspectives)*, Paris, France, 6–11 September, 2009; pp 1127–1132.
(56) J.-M. Adnet, M. Miguirditchian, C. Hill, X. Hérès, M. Lecomte, M. Masson, P. Brossard, and P. Baron, Development of new hydrometallurgical processes for actinide recovery: GANEX concept. In *Proc. Internat. Conf. GLOBAL 2005 (Nuclear Energy Systems for Future Generation and Global Sustainability)*, Tsukuba, Japan, 9–13 October, 2005.
(57) B. Weaver, and F. A. Kappelmann, TALSPEAK: A New Method of Separating Americium and Curium from the Lanthanides by Extraction from am Aqueous Solution of an Aminopolyacetic Acid Complex with a Monoacidic Organophosphate or Phosphonate. ORNL-3559, Oak Ridge National Laboratory, USA, 1964.
(58) K. L. Nash, *Solv. Extr. Ion Exch.*, 2015, **33**, 1.
(59) Y. Sasaki, Y. Sugo, S. Suzuki, S. Tachimori, *Solvent Extr. Ion Exch.,* 2001, **19,** 91.
(60) G. V. Buxton, C. L. Greenstock, W. P. Helman, and A. B. Ross, *J. Phys. Chem. Ref. Data* **1988**, 17, 513–886.
(61) H. Galan, D. Munzel, A. Nunez, U. Mullich, J. Cobos, and A. Geist, A. Stability and Recyclability of SO3-Ph-BTP for *i*-SANEX Process Development, ISEC2014 International Solvent Extraction Conference, September 7 – 11, 2014, Wurzberg, Germany, 2014.
(62) P. Y. Jiang, Y. Katsumura, K. Ishigure, and Y. Yoshida, *Inorg. Chem.*, 1992, ***31 (24)***, 5135.
(63) S. M. Pimblott and J. A. LaVerne, *J. Phys. Chem. A*, 1998, **102**, 2967.
(64) T. Logager and K. Sehested, *J. Phys. Chem.*, 1993, **97**, 6664.
(65) M. Graetzel, A. Henglein, and S. Taniguchi, *Ber. Bunsenges. Phy. Chem.*, 1970, **74**, 292.
(66) M. Graetzel, A. Henglein, J. Lilie, and G. Beck, *Ber. Bunsenges. Phy. Chem.*, 1969, **73**, 646.
(67) G. Lammel, D. Perner, and P. Warneck, *J. Phys. Chem.*, 1990, **94**, 6141.
(68) Y. Katsumura, N-Centered Radicals, the Chemistry of Free Radicals, John Wiley & Sons, Chichester 1998.
(69) D. Peterman, A. Geist, B. Mincher, G. Modolo, M. H. Galan, L. Olson, and R. McDowell, *Ind. Eng. Chem. Res.*, 2016, **55**, 10427.
(70) G.L. Traister, A.A. Schilt, *Anal. Chem.,* 1976, **48,** 1216.
(71) H. Fricke and E. J. Hart, *J. Chem. Phys.*, 1935, **3**, 60.
(72) K. Whitman, S. Lyons, R. Miller, D. Nett, P. Treas, A. Zante, R. W. Fessenden, M. D. Thomas, and Y. Wang, Linear Accelerator for Radiation Chemistry Research at Notre Dame. *Proceedings of the '95 Particle Accelerator Conference and International Conference on High Energy Accelerators, Texas, USA*. 1996.
(73) G. L. Hug, Y. Wang, C. Schöneich, P. Y. Jiang, and R. W. Fessenden, *Radiat. Phys. Chem.*, 1999, **54**, 559.
(74) G. V. Buxton and C. R. Stuart, *J. Chem. Soc. Faraday Trans.*, 1995, **92**, 279.
(75) A. J. Elliot and D. M. Bartels, The Reaction Set, Rate Constants and G-Values for the Simulation of the Radiolysis of Light Water Over the Range 20° to 350°C Based on Information Available in 2008. *AECL Nuclear Platform Research and Development – Report 153-127160-450-001*. 2009.
(76) S. M. Pimblott and J. A. LaVerne, *Rad. Res.*, 1993, **135**, 16.
(77) B. J. Mincher and R. D. Curry, *Applied Radiation and Isotopes*, 2000, **52 (2)**, 189.
(78) D. Magnusson, B. Christiansen, R. Malmbeck, and J. P. Glatz, *Radiochim. Acta*, 2009, **97 (9)**, 497.
(79) S. P. Mezyk and S. C. Otto, *J. Adv. Oxidat. Technol.*, 2013, **16 (1)**, 117.
(80) S. Gordon, E. J. Hart, M. S. Matheson, J. Rabani, and K. J. Thomas,

*Discuss. Faraday. Soc., 1963, **36**, 193.*
(81) F. W. Lewis, L. M. Harwood, M. J. Hudson, A. Nunez, H. Galan, and A. G. Espartero, *Synlett*, 2016, **27**, 1.
(82) E. Macerata, E. Mossini, S. Scaravaggi, M. Mariani, A. Mele, W. Panzeri, N. Boubals, L. Berthon, M.-C. Charbonnel, F. Sansone, A. Arduini, A. Casnati, *J. Amer. Chem. Soc.,* 2016, **138**, 7232.